Inhibitors of PI(4,5)P$_2$ Synthesis Reveal Dynamic Regulation of IgE Receptor Signaling by Phosphoinositides in RBL Mast Cells[S]

Marcela de Souza Santos, Rose Mary Zumstein Georgetto Naal, Barbara Baird, and David Holowka

Departamento de Física e Química, Faculdade de Ciências Farmacêuticas de Ribeirão Preto, Universidade de São Paulo, São Paulo, Brazil (M.S.S., R.M.Z.G.N.); Department of Chemistry and Chemical Biology, Cornell University, Ithaca, New York (B.B., D.H.)

ABSTRACT

Phosphatidylinositol 4,5-bisphosphate (PI(4,5)P$_2$) is a versatile phospholipid that participates in many membrane-associated signaling processes. PI(4,5)P$_2$ production at the plasma membrane (PM) depends on levels of its precursor, phosphatidylinositol 4-phosphate (PI4P), synthesized principally by two intracellular enzymes, PI4-kinases IIIα and IIIb; the former is preferentially inhibited by phenylarsine oxide (PAO). We found that PAO and quercetin, another lipid kinase inhibitor, rapidly inhibit Ca^{2+} responses to antigen in IgE-sensitized rat basophilic leukemia mast cells. Quercetin also rapidly inhibits store-operated Ca^{2+} influx stimulated by thapsigargin. In addition, quercetin and PAO effectively inhibit antigen-stimulated ruffling and spreading in these cells, and they inhibit endocytosis of crosslinked IgE receptor complexes, evidently by inhibiting pinching off of endocytic vesicles containing the clustered IgE receptors. A minimal model to account for these diverse effects is inhibition of PI(4,5)P$_2$ synthesis by PAO and quercetin. To characterize the direct effects of these agents on PI(4,5)P$_2$ synthesis, we monitored the reappearance of the PI(4,5)P$_2$-specific PH domain PH-phospholipase C δ-EGFP at the PM after Ca^{2+} ionophore (A23187)-induced PI(4,5)P$_2$ hydrolysis, followed by Ca^{2+} chelation with excess EGTA. Resynthesized PI(4,5)P$_2$ initially appears as micron-sized patches near the PM. Addition of quercetin subsequent to A23187-induced PI(4,5)P$_2$ hydrolysis reduces PI(4,5)P$_2$ resynthesis in PM-associated patches, and PAO reduces PI(4,5)P$_2$ at the PM while enhancing PI(4,5)P$_2$ accumulation at the Golgi complex. Taken together, these results provide evidence that PI4P generated by PI4-kinase IIIα is dynamically coupled to PI(4,5)P$_2$ pools at the PM that are important for downstream signaling processes activated by IgE receptors.

Introduction

Phosphatidylinositol 4,5-bisphosphate [PI(4,5)P$_2$] constitutes only about 1% of total plasma membrane phospholipids, but it has been found to play important roles in a large number of cellular processes. PI(4,5)P$_2$ was established as a second messenger in signal transduction pathways by Berridge and coworkers (1983), who showed that agonist-stimulated activation of phospholipase C (PLC) resulted in cleavage of PI(4,5)P$_2$ to generate inositol 1,4,5-trisphosphate (IP$_3$) and diacylglycerol (DAG). PI(4,5)P$_2$ was subsequently shown to serve as a substrate for phosphatidylinositol 3-kinase during the synthesis of phosphatidylinositol 3,4,5-trisphosphate [PI(3,4,5)P$_3$], a key player for cell proliferation, migration, chemotaxis, phagocytosis, differentiation, survival, and metabolical changes (Cantley, 2002). PI(4,5)P$_2$ has been implicated in the control of many processes, including vesicular trafficking, membrane dynamics, actin cytoskeleton organization, activation of ion channels and transporters (Di Paolo and De Camilli, 2006; Balla et al., 2009). Given its extraordinary versatility in cellular signaling, it is likely that PI(4,5)P$_2$ may exist as spatially and functionally distinct pools in the cell (Johnson et al., 2008; Vasudevan et al., 2009; Calloway et al., 2011).

Mast cells are key effector cells in IgE-associated immune responses, including allergic disorders and protective immune responses against certain bacteria and parasites (Beaven, 2009). Mast cells carry out adaptive immune functions through antigen- and IgE-dependent clustering of the high-affinity IgE receptor FcεRI (Holowka et al., 2007). Crosslinking of IgE-FcεRI complexes at the mast cell surface initiates a signaling cascade that causes mast cell activation, resulting in Ca^{2+} mobilization and consequent release of preformed and newly synthesized mediators of the allergic response and inflammation (Rivera and Gilfillan, 2006). The rat basophilic leukemia

ABBREVIATIONS: BSA, bovine serum albumin; BSS, buffered salt solution; DAG, diacylglycerol; ER, endoplasmic reticulum; IP$_3$, inositol 1,4,5-trisphosphate; MARCKS, myristoylated alanine-rich protein kinase C substrate; PAO, phenylarsine oxide; PI(3,4,5)P3, phosphatidylinositol 3,4,5-trisphosphate; PI(4)P, phosphatidylinositol 4-phosphate; PI(4,5)P$_2$, phosphatidylinositol 4,5-bisphosphate; PI4K, phosphatidylinositol 4-kinase; PKC, protein kinase C; PLC, phospholipase C; PM, plasma membrane; RBL, rat basophilic leukemia; SOCE, store-operated Ca^{2+} entry.

(RBL)-2H3 mast cell line has structural and functional characteristics similar to differentiated mucosal mast cells (Seldin et al., 1985; Lee et al., 2012), and it has been used extensively for biochemical and cell biologic investigations of mast cell function (Passante and Frankish, 2009). Antigen-mediated crosslinking of IgE-FcεRI complexes initiates Lyn kinase-mediated tyrosine phosphorylation of FcεRI immunoreceptor tyrosine-based activation motifs, resulting in recruitment and activation of Syk tyrosine kinase that, in turn, phosphorylates several downstream targets, including PLCγ. This phosphorylation activates PLCγ to hydrolyze PI(4,5)P$_2$ and generate IP$_3$ and DAG; IP$_3$ binds to its receptor at the endoplasmic reticulum (ER) to trigger the release of Ca^{2+} from ER stores, which activates store-operated Ca^{2+} entry (SOCE), and DAG participates with Ca^{2+} mobilization to activate protein kinase C (PKC). These signals synergize to activate mast cell degranulation for release of a number of preformed allergic mediators, as well as for the de novo synthesis and secretion of various cytokines that together mediate the early and late phases of allergic reactions (Rivera and Gilfillan, 2006).

Recent studies from our laboratory have highlighted roles for PI(4,5)P$_2$ in mast cell activation. Vasudevan et al. (2009) provided evidence that two different isoforms of type I phosphatidylinositol 4-phosphate 5-kinase synthesize functionally different pools of PI(4,5)P$_2$ at the PM that play distinct roles in antigen-stimulated IP$_3$ production and SOCE. More recently, Calloway et al. (2011) found that the ratio of PI(4,5)P$_2$ associated with detergent-resistant, ordered lipids to that associated with detergent-solubilized, disordered lipids regulates coupling of the ER sensor protein STIM1 with the Ca^{2+} channel protein Orai1 during SOCE (Calloway et al., 2011). Furthermore, Gadi et al. (2011) showed that the polybasic effector domain of the PKC substrate MARCKS (myristoylated alanine-rich protein kinase C substrate), mutated to prevent PKC-mediated dissociation from phosphoinositide binding at the PM, results in delayed Ca^{2+} mobilization and inhibition of mast cell degranulation to implicate PI(4,5)P$_2$ in these processes.

The limiting pool of PI(4,5)P$_2$ needs continuous replenishment. In mammalian cells, phosphatidylinositol 4-phosphate [PI(4)P] is at least 50 times more abundant than PI(5)P, and it is generally accepted that the majority of PI(4,5)P$_2$ derives from phosphorylation of PI(4)P (Di Paolo and De Camilli, 2006). Pharmacologic inhibitors of phosphoinositide synthesis have been used to characterize this dynamic turnover in limited contexts (Balla and Balla, 2006). In the present study we characterize the use of two inhibitors of PI4-kinases and PI5-kinases to inhibit new synthesis of PI(4,5)P$_2$ in RBL mast cells and to provide evidence for roles of these phosphoinositides in FcεRI signaling. We found that both phenylarsine oxide (PAO) and quercetin [2-(3,4-dihydroxyphenyl)-3,5,7-trihydroxy-4*H*-chromen-4-one] acutely inhibit antigen-stimulated cellular responses, including Ca^{2+} release from ER stores and SOCE, membrane ruffling and cell spreading, and endocytosis of IgE-FcεRI. Our results provide evidence for synthesis of PI(4,5)P$_2$ in novel PM-proximal micron-sized domains in a process that is sensitive to inhibition by PAO and quercetin. Our findings can be accounted for by a model in which PAO inhibits FcεRI signaling primarily by inhibition of PI4P synthesis, and quercetin more directly inhibits PI(4,5)P$_2$ synthesis by inhibiting PI5-kinases.

Materials and Methods

Cell Culture. RBL-2H3 cells were cultured as monolayers in minimal essential medium (Invitrogen Corp., Carlsbad, CA) with 20% fetal bovine serum (Atlanta Biologicals, Atlanta, GA) and 10 μg/ml gentamicin sulfate (Invitrogen). Unless otherwise specified, other reagents were from Sigma-Aldrich (St. Louis, MO).

Ca^{2+} Measurements. Cytoplasmic Ca^{2+} levels were measured using an SLM 8100C steady-state fluorimeter (SLM Instruments, Urbana, IL). Cells suspended in buffered salt solution (BSS: 135 mM NaCl, 5 mM KCl, 1 mM MgCl$_2$, 1.8 mM CaCl$_2$, 5.6 mM D(+) glucose, 20 mM HEPES, pH 7.4) were loaded with 0.5 μM Ca^{2+} indicator Fluo-4 AM (excitation 490 nm, emission 520 nm; Invitrogen) and sensitized with 2 mg/ml anti-DNP IgE (purified as previously described, Posner et al., 1992) in BSS with 0.5 mM sulfinpyrazone and 1 mg/ml bovine serum albumin (BSA). Cells were stimulated with 0.4 μg/ml DNP-BSA or 0.2 μM thapsigargin, and quercetin, PAO, or gadolinium chloride were added as indicated. Cells were lysed by the addition of 0.1% Triton X-100 to obtain the maximum value of Fluo-4 fluorescence, which was subsequently quenched with 6 mM EGTA to determine background Fluo-4 fluorescence values.

Ruffling and Spreading Assay. Cells were plated at a subconfluent density of 0.5×10^6 cells/ml in 35-mm coverslip dishes (MatTek Corporation, Ashland, MA) and sensitized with anti-DNP IgE overnight. Cells were incubated for 2 minutes with either 20 μM quercetin or 2 μM PAO, followed by stimulation with DNP-BSA (0.5 μg/ml) during 10 minutes at 37°C. Cells were fixed in 4% paraformaldehyde and 0.1% glutaraldehyde, quenched with 10 mg/ml BSA in PBS with 0.01% sodium azide, then permeabilized with 0.1% Triton X-100 and labeled for F-actin with Alexa fluor 568-phalloidin (Invitrogen) to visualize cell ruffling (dorsal cell surface) and spreading (ventral cell surface). To quantify cell ruffling, 200–300 cells from multiple experiments were scored for ruffling. To quantify cell spreading, cell body area was outlined and measured using the software ImageJ (NIH) for 20 cells per sample in each of 3 independent experiments.

Measurements of IgE-FcεRI Surface Accessibility, Localization, and Acidification Changes by Antigen. For measurement of IgE-FcεRI surface accessibility before and after crosslinking, RBL-2H3 cells in suspension (5×10^6 cell/ml) were sensitized with 4 μg/ml of Alexa fluor 488-IgE (A488-IgE) for 45 minutes at 37°C. Sensitized cells were washed and resuspended in BSS, incubated in the presence or absence of 2 μM PAO or 20 μM quercetin for 2 minutes, then antigen (0.4 μg/ml) was added for 20 minutes at 37°C. Cells were chilled at 4°C, washed, and incubated for 60 minutes with rabbit anti-Alexa fluor 488 Ab (1:1000 dilution; Invitrogen/Molecular Probes), then washed and labeled at 4°C with Cy5-conjugated goat anti-rabbit Ab (1:500 dilution; Invitrogen). Labeled cells were fixed with 4% paraformaldehyde and 0.1% glutaraldehyde for 20 minutes, room temperature, then resuspended in PBS/sodium azide with 10 mg/ml BSA, and the Cy5 label was quantified by flow cytometry.

For subcellular localization of IgE-FcεRI under conditions similar to those described above, adherent cells were plated overnight at ~0.5×10^6 cells/ml in 35-mm coverslip dishes (MatTek), then sensitized with A488-IgE for 2 hours at 37°C. Cells were preincubated with or without 2 μM PAO or 20 μM quercetin for 5 minutes, followed by antigen stimulation for 10 minutes at 37°C and fixation as described above. Fixed cells were labeled with anti-Alexa fluor 488 Ab as above and then with Alexa fluor 555-labeled goat anti-rabbit IgG (1:200 dilution; Invitrogen). Distributions of Alexa fluor 488 and Alexa fluor 555 label were visualized using a Zeiss 710 laser scanning confocal system (Jena, Germany) with a 63× 1.1 NA oil-immersion objective.

For measurement of IgE-FcεRI acidification due to endocytosis, RBL mast cells in suspension were sensitized with 5 μg/ml FITC-IgE for 1 hour at 37°C, washed, and resuspended in BSS for steady-state monitoring of FITC fluorescence as previously described (Menon et al., 1986). In the fluorimeter, stirred cells were treated with 2 μM PAO or 20 μM quercetin followed by rabbit anti-IgE (1:200 dilution) at 37°C for time-dependent measurements of FITC fluorescence.

Measurements of PI(4,5)P$_2$ Synthesis at the Plasma Membrane. Cells plated in 35 mm MatTek dishes were cultured overnight for subsequent transfection with the PI(4,5)P$_2$-specific construct PH-PLCδ1-EGFP (2 μg/ml; Várnai and Balla, 1998), using FuGENE HD (8 μl/ml; Roche Diagnostics, Germany) in OptiMEM (Invitrogen). Cells were incubated with the DNA-FuGENE complexes for 1 hour, then 0.1 μM phorbol 1,2-dibutyrate (Sigma-Aldrich) was added to the cells for 4 hours to enhance fluid phase pinocytosis and DNA uptake. About 24 hours after transfection and prior to imaging, cells were washed with BSS and the dishes were placed on a heated stage with controlled temperature of 37°C. Cells were incubated with 1.5 ml BSS for acquisition of images using confocal microscopy. Live images were acquired every 13 seconds during a time period of ~25 minutes before and after cell stimulation with the Ca^{2+} ionophore A23187 (10 μM), followed by quercetin (20 μM) or PAO (2 μM), then 2 mM EGTA. To quantify the ratio of PH-PLCδ1-EGFP at the plasma membrane to that in the cytoplasm, line scans were analyzed using ImageJ (NIH, Bethesda, MD) (Smith et al., 2010). For cells with PM-associated patches, line scans were chosen to bisect patches with representative intensities.

Results

Pharmacologic Inhibitors of Phosphoinositide Synthesis Inhibit Stimulated Ca^{2+} Responses in Mast Cells. A previous study showed that micromolar concentrations of phenylarsine oxide (PAO) caused a modest enhancement of antigen-stimulated tyrosine phosphorylation of multiple proteins in RBL mast cells, consistent with its capacity to inhibit tyrosine phosphatases (Adamczewski et al., 1992). Somewhat surprisingly, PAO also selectively inhibited antigen-stimulated tyrosine phosphorylation of PLCγ1, and in parallel it inhibited Ca^{2+} mobilization and consequent degranulation with a dose dependence in the low micromolar range. Subsequently, Wiedemann and colleagues (1996) demonstrated inhibition of PI4-kinase (PI4K) enzyme activity by both PAO and quercetin, a bioflavonoid, with concomitant loss of PI(4)P and PI(4,5)P$_2$ pools and a correlative loss of the stimulated secretory responsiveness of chromaffin cells. PAO has been found to inhibit type III PI4-kinases, with relatively little effects on type II PI4K enzymes, and, among the type III enzymes, PI4KIIIα is more sensitive to PAO than PI4K IIIβ (Balla et al., 2002). Quercetin is a well-known natural flavonol (Chirumbolo, 2010) that has been found to inhibit PI kinases and other kinases by competition with ATP for the active site (Middleton et al., 2000). Its capacity to inhibit IgE receptor-mediated mast cell degranulation was previously established (Fewtrell and Gomperts, 1977), but the mechanism of this inhibition was not determined. We confirmed this dose-dependent inhibition for RBL-2H3 cells in the present study (Supplemental Fig. 1).

It has long been recognized that functional responses of mast cells, such as degranulation, that are stimulated by antigen-mediated FcεRI activation require sustained levels of cytoplasmic Ca^{2+} (Ma and Beaven, 2009). Antigen-stimulated activation of PLCγ results in IP$_3$-mediated depletion of ER Ca^{2+} stores that activates SOCE via Ca^{2+} release-activated Ca^{2+} channels (Vig and Kinet, 2009). To investigate the mechanisms by which PAO and quercetin inhibit FcεRI-mediated Ca^{2+} responses in RBL mast cells, we monitored Ca^{2+} levels in suspended cells using the Ca^{2+} indicator Fluo-4 and steady-state fluorimetry. As shown in Fig. 1A, left panel, antigen stimulation of RBL cells causes a robust increase in cytoplasmic Ca^{2+}, and addition of 1 μM PAO after several minutes of stimulation results in rapid inhibition of the stimulated Ca^{2+} response, with little further effect by subsequent additions of 10 μM quercetin or 1 μM Gd^{3+}. The latter is an effective inhibitor of SOCE in these cells (Calloway et al., 2011). In other experiments, addition of higher concentrations of PAO did not substantially increase the inhibition of Ca^{2+} responses observed (unpublished data). Sustained increases in Ca^{2+} in response to antigen or the SERCA ATPase inhibitor, thapsigargin, are maintained for at least 10 minutes in the absence of PAO, quercetin, or other inhibitors (Supplemental Fig. 2).

Similar to the effect of PAO on antigen-stimulated Ca^{2+} mobilization, addition of quercetin at a final concentration of 10 μM caused rapid inhibition of this response, which was not further inhibited by additions of PAO or Gd^{3+} (Fig. 1A, right panel). The baseline drift in this experiment is due to leakage of the indicator dye, Fluo-4, from these cells; it is minimized by inclusion of sulfinpyrazone (0.5 mM) in the buffer, but this inhibition is somewhat variable from day-to-day (compare baselines in Fig. 1, A and B). Taken together, these results suggest that PAO and quercetin are inhibiting the same or overlapping molecular targets.

Calloway et al. (2011) provided evidence that, in addition to serving as a substrate for PLC in the generation of IP$_3$-mediated Ca^{2+} influx, PI(4,5)P$_2$ plays a role in regulating SOCE stimulated by thapsigargin. As shown in Fig. 1B, thapsigargin-induced SOCE was not inhibited by acute addition of 1 μM PAO after several minutes of stimulation, but this response is substantially inhibited by two successive additions of 10 μM quercetin, with no additional inhibition by 1 μM Gd^{3+}. Results from multiple experiments such as those in Fig. 1, A and B, are summarized in Fig. 1C. They show that antigen-stimulated Ca^{2+} responses are rapidly inhibited by both quercetin and PAO, and they show that SOCE activated downstream of IP$_3$-dependent release of Ca^{2+} from ER stores is sensitive to acute inhibition by quercetin but not PAO. In other experiments, however, we found that addition of 1 μM PAO for at least 10 minutes prior to stimulation by thapsigargin results in substantial inhibition of SOCE (Supplemental Fig. 3; see *Discussion*). Similarly, we previously found that preincubation of RBL cells with 10 μM wortmannin (but not acute addition) resulted in ~40% inhibition of thapsigargin-stimulated SOCE, consistent with inhibition by depletion of PI4P (Calloway et al., 2011).

PAO was previously shown to effectively inhibit antigen-stimulated PI turnover, providing evidence for its capacity to inhibit IP$_3$-dependent Ca^{2+} release from stores (Adamczewski et al., 1992). To determine more directly whether quercetin inhibits Ca^{2+} mobilization by inhibiting antigen-stimulated Ca^{2+} release from stores, we examined the Ca^{2+} response to antigen in the absence of extracellular Ca^{2+}. Under these conditions, the transient Ca^{2+} response observed depends on IP$_3$-mediated Ca^{2+} release from the ER stores (Lee et al., 2005). Fig. 1D clearly shows that the Ca^{2+} transient generated upon antigen stimulation is strongly inhibited when cells are pretreated with 20 μM quercetin, consistent with an effect of quercetin on PLC activation and/or phosphoinositide synthesis. The capacity of quercetin to inhibit thapsigargin-stimulated SOCE (Fig. 1, B and C) is not likely to be due to inhibition of PLC activation but is accountable by inhibition of phosphoinositide synthesis.
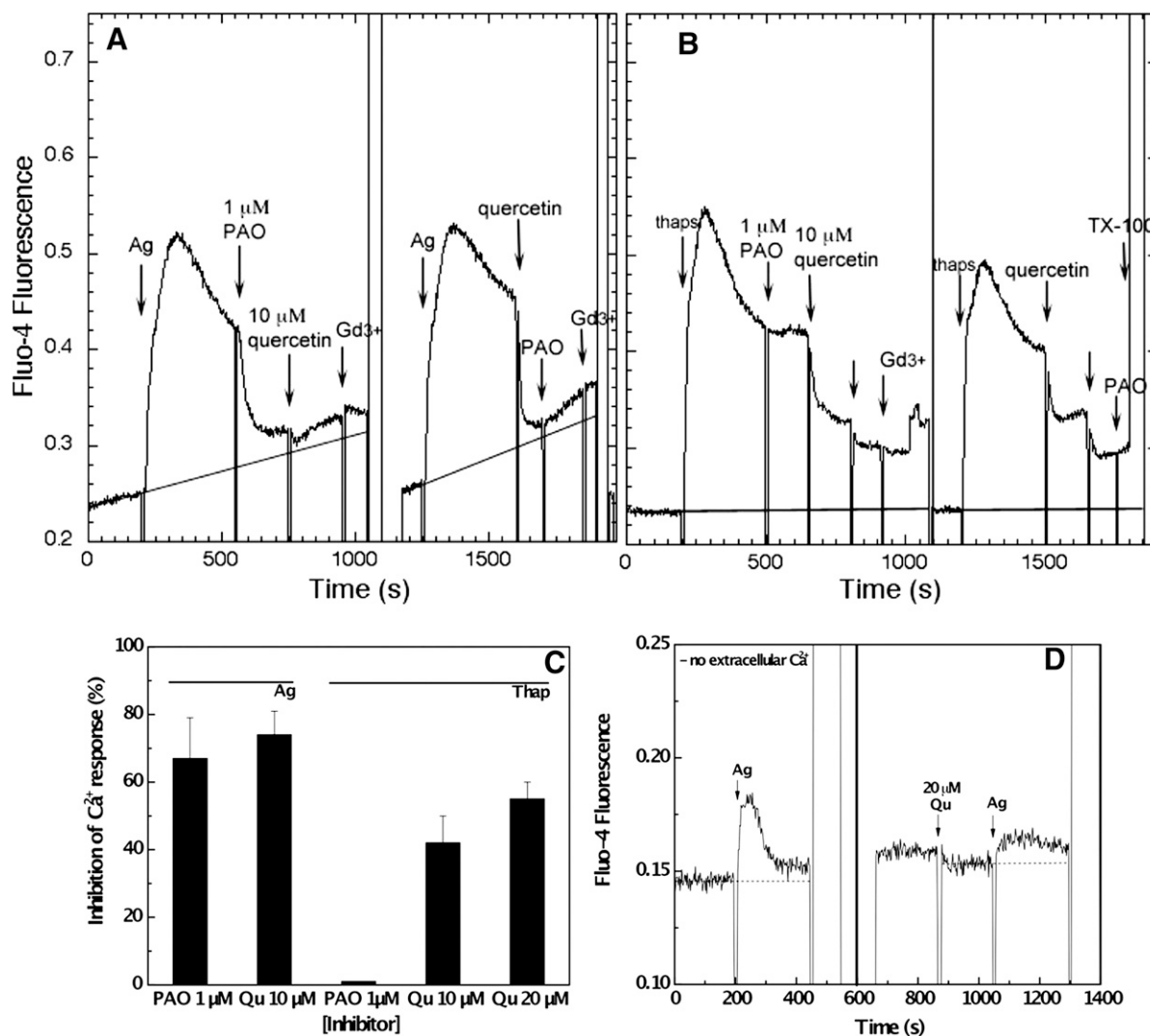
Fig. 1. Rapid inhibition of Ca^{2+} mobilization by PAO and quercetin. RBL mast cells, sensitized with anti-DNP IgE and loaded with Fluo-4, were stimulated either with Ag (A) or thapsigargin (thaps) (B) and further treated with 1 μM PAO, 10 μM quercetin, and 1 μM Gd^{3+} as indicated. Unlabeled arrows indicate additions identical to previous. Two separate experiments are shown in each panel. (C) Quantitative representation of inhibition of Ag and thaps-stimulated Ca^{2+} responses by PAO and quercetin (Qu) in three independent experiments $\pm$ S.D. (D) Representative experiment showing inhibition of Ca^{2+} release by quercetin in the absence of extracellular Ca^{2+}. The decrease in Fluo-4 fluorescence upon addition of quercetin represents a small amount of nonspecific fluorescence quenching.

Considering that quercetin has been shown to inhibit a variety of kinases other than phosphatidylinositol kinases (Middleton et al., 2000), we investigated whether its inhibitory effect on antigen-induced Ca^{2+} mobilization could be attributed to inhibition of tyrosine phosphorylation stimulated by antigen-mediated FcεRI crosslinking. As shown in Supplemental Fig. 4, quercetin caused some inhibition of both the Lyn-dependent phosphorylation of FcεRI β subunit (Paolini et al., 1991) and the Syk-dependent phosphorylation of pp72 (Benhamou et al., 1993), but only at the higher range of the concentrations used in this study, and such inhibition was not statistically significant. At 10 μM quercetin, antigen-stimulated Ca^{2+} mobilization is substantially inhibited (Fig. 1A), but no inhibition of antigen-stimulated tyrosine phosphorylation is detected (Supplemental Fig. 3).

Quercetin and PAO Inhibit Antigen-Stimulated Morphologic Changes in RBL Mast Cells. In addition to stimulating release of preformed and newly synthesized

allergic mediators, crosslinking of FcεRI receptors by multivalent antigen is known to result in increased actin polymerization and membrane ruffling. For attached cells, FcεRI-mediated activation also results in cell flattening and spreading (Pfeiffer et al., 1985). Actin cytoskeleton-PM interactions are the driving force to the formation and retraction of lamellipodia (ruffles), filopodia, and adhesion in response to chemoattractants and other stimuli (Raucher et al., 2000). The capacities of PI(4,5)P$_2$ to regulate actin-associated proteins underlie the importance of this phosphoinositide in determining the interactions between the PM and the actin cytoskeleton (Johnson et al., 2008). Because of this, we explored the effects of PAO and quercetin on morphologic changes induced by FcεRI crosslinking in RBL cells. As described previously (Pfeiffer et al., 1985), antigen-mediated RBL mast cell activation causes these cells to transform from exhibiting a fine microvillous surface to dramatic ruffles, as depicted in Fig. 2A (upper panel) by confocal
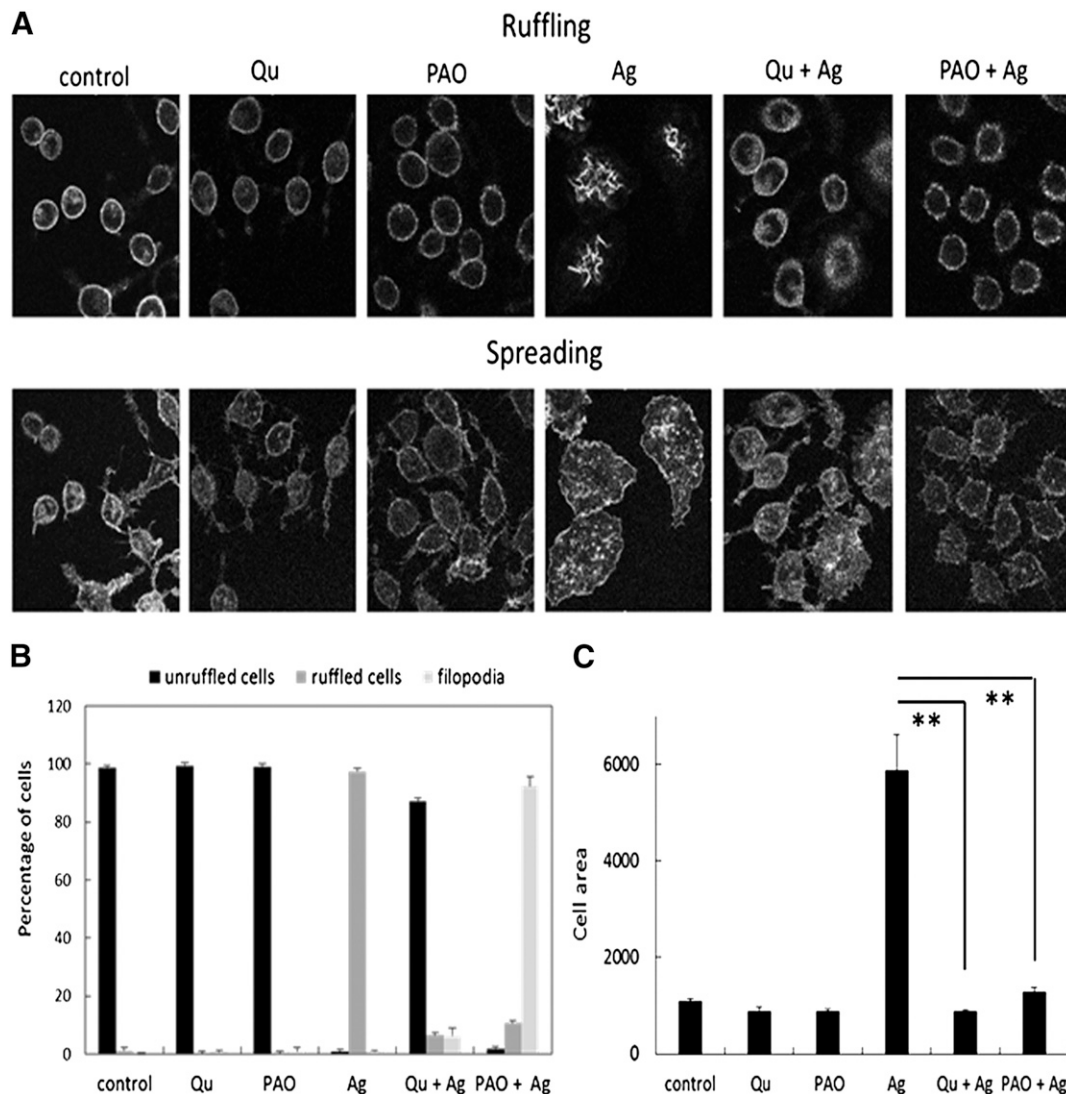
A

Ruffling

Spreading

B

C

Fig. 2. Ag-stimulated cell ruffling and spreading are inhibited by PAO and quercetin. (A) IgE-sensitized cells were pretreated with or without quercetin (20 μM) or PAO (2 μM) for 2 minutes and then stimulated with Ag (DNP-BSA, 0.5 μg/ml) for 10 minutes. Cells were then fixed and labeled for F-actin with A568-phalloidin for analysis by confocal microscopy. Cells were scored for ruffling (B) and cell area for spreading (C) for >50 cells for each condition in three independent experiments (error bars represent S.D.). The difference between the cell area among Ag-stimulated cells with or without inhibitors was statistically analyzed using Student's t test and was considered significant when **$P < 0.01$.

microscopy images of Alexa fluor 568-phalloidin-labeled F-actin focused at the dorsal cell surface. Incubation with quercetin for several minutes did not alter the morphology of unstimulated cells, but this addition prior to antigen stimulation prevented the development of ruffles for the vast majority of the cells (Fig. 2A, upper panel). Incubation with PAO also had no effect on the morphology of unstimulated cells, but antigen stimulation in the presence of PAO generated filopodia rather than the dramatic ruffles of the control cells (Fig. 2A, upper panel). Quantitative enumeration of these phenotypes is summarized in Fig. 2B.

Confocal microscopy images focused at the cell-substrate interface reveal enhanced spreading of antigen-activated cells in comparison with unstimulated cells (Fig. 2A, bottom panel). These images, together with quantitative measurements of cell area of more than 50 cells per sample summarized in Fig. 2C, show that both PAO and quercetin inhibit antigen-stimulated cell spreading. In addition, both

of these compounds reduce the appearance of intensely fluorescent F-actin plaques at the ventral surface of antigen-stimulated cells. Such plaques have been demonstrated to be involved in mast cell adherence to the substratum, which has been shown to enhance degranulation (Hamawy et al., 1992).

Together, our results show that both PAO and quercetin strongly attenuate antigen-induced morphologic changes in RBL mast cells. As antigen-stimulated morphologic changes are not dependent on stimulated Ca^{2+} influx (Pfeiffer et al., 1985; Naal et al., 2003), the results imply that PAO and quercetin inhibit a process necessary for the morphologic changes in addition to their effects on Ca^{2+} mobilization. A process important for both Ca^{2+} mobilization and stimulated morphologic changes is phosphoinositide synthesis.

Quercetin and PAO Inhibit Crosslink-dependent Endocytosis of Ige-FcεRIH. PI(4,5)P$_2$ has been shown to be important in clathrin-mediated endocytosis (Zoncu et al.,

2007), but its role in IgE receptor endocytosis in response to antigen is unknown. To investigate this question we first monitored the surface accessibility of Alexa488-conjugated IgE (A488-IgE) using anti-Alexa488 Ab and a Cy5-conjugated secondary antibody with flow cytometry. A488-IgE is localized to the cell surface in the absence of antigen, and its surface accessibility is reduced by ~65% following antigen-mediated FcεRI crosslinking for 20 minutes at 37°C (Fig. 3A). When internalization was inhibited by crosslinking with antigen at 4°C, accessibility to anti-Alexa488 was reduced less than 5% (A. Singhai and D. Holowka, unpublished data). Addition of either 2 μM PAO or 20 μM quercetin did not alter the accessibility of A488-IgE prior to crosslinking by antigen, and they did not significantly affect the antigen-dependent loss of A488-IgE accessibility to anti-Alexa488 at 37°C (Fig. 3A).
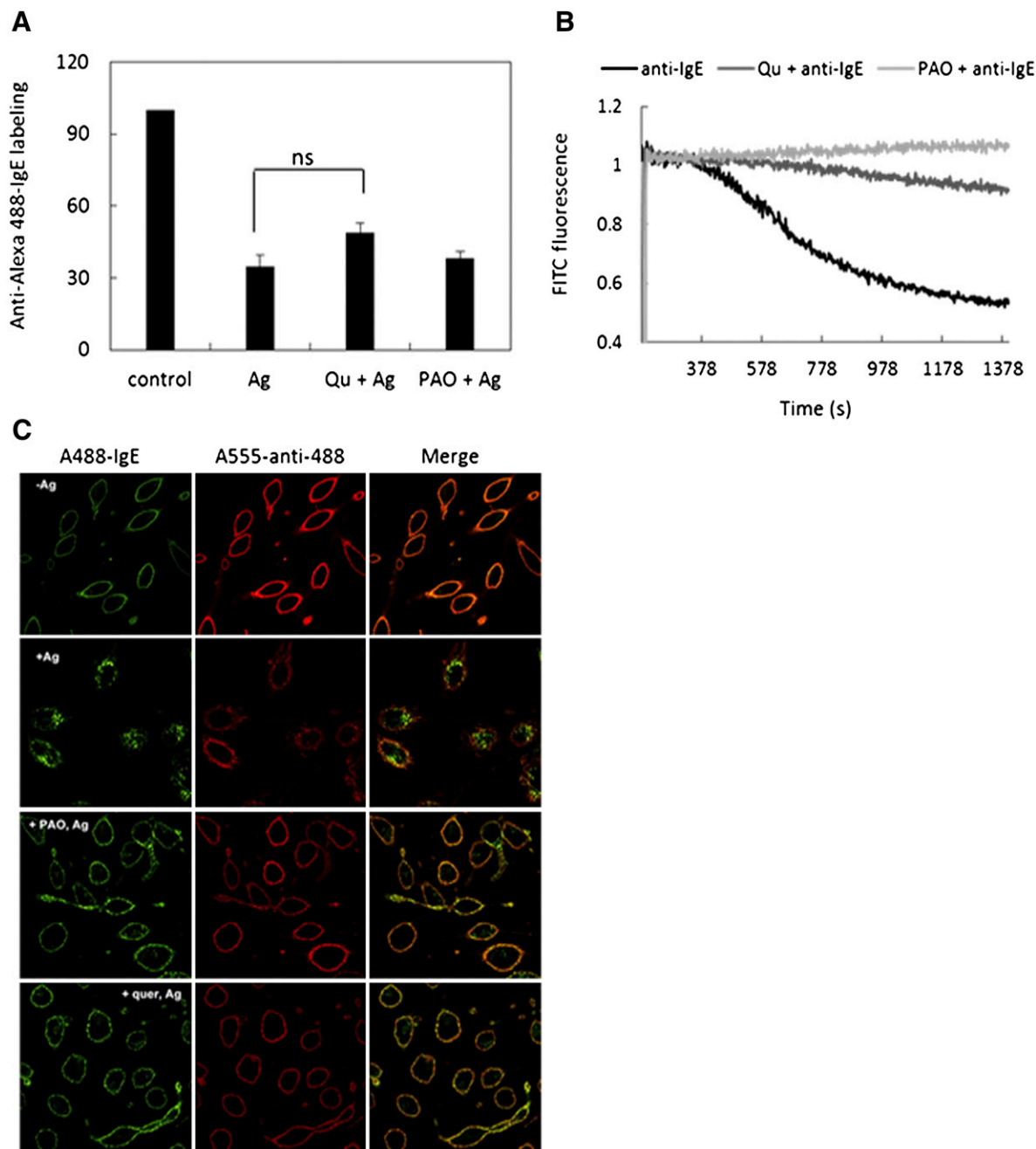

Fig. 3. Quercetin and PAO inhibit acidification and pinching off of crosslinked IgE/FcεRI complexes. (A) A488-IgE-sensitized RBL cells in suspension were pretreated or not with 20 μM quercetin or 2 μM PAO for 2 minutes, followed by IgE/FcεRI crosslinking by antigen at 37°C. Cells were then chilled to 4°C and labeled with anti-A488 Ab and Cy5-conjugated secondary Ab prior to fixation. Accessibility of A488-IgE at the cell surface was assessed by flow cytometry measurements of Cy5 fluorescence. (B) Suspended RBL cells were sensitized with FITC-IgE, washed, then treated or not with 20 μM quercetin or 2 μM PAO for 5 minutes prior to crosslinking of IgE/FcεRI complexes by anti-IgE at t = 0. Acidification of internalized complexes was monitored by FITC-IgE fluorescence quenching. (C) Attached RBL cells sensitized with Alexa 488-IgE were treated or not with 20 μM quercetin or 2 μM PAO for 5 minutes prior to addition of Ag (DNP-BSA 0.5 μg/ml) for 10 minutes at 37°C. Following fixation, surface accessibility of IgE was detected by labeling with anti-A488 and A555-anti-rabbit Ab and imaged by confocal microcopy.

IgE receptors internalized by crosslinking undergo trafficking to lysosomes, where they are proteolytically degraded (Furuichi et al., 1986). Because late endosomes and lysosomes are acidic (pH 4.5–5.5) (Sorkin and Von Zastrow, 2002), this trafficking can be monitored using a fluorescent indicator (fluorescein) conjugated to IgE (FITC-IgE) (Menon et al., 1986). Thus, we monitored time-dependent changes in FITC-IgE fluorescence in response to IgE-FcεRI crosslinking. For this experiment we used anti-IgE to crosslink FITC-IgE to avoid the substantial quenching of FITC-IgE caused by DNP-BSA binding. As shown in Fig. 3B, we observed a time-dependent decrease in FITC fluorescence following addition of anti-IgE to FITC-IgE-sensitized cells. Brief preincubation of these cells with 2 μM PAO or 20 μM quercetin did not alter the FITC-IgE fluorescence, but these compounds substantially reduced FITC quenching due to anti-IgE crosslinking in this representative experiment, indicating that inaccessible FITC-IgE-receptor complexes (Fig. 3A) were not becoming acidified under these conditions. As endocytosis and subsequent acidification is a Ca^{2+}-independent process (Furuichi et al., 1984), it is unlikely that the capacity of these compounds to inhibit endosomal acidification depends on their capacity to inhibit Ca^{2+} mobilization.

To gain insight into how PAO and quercetin inhibit crosslink-dependent acidification while permitting loss of accessibility to anti-Alexa488 Ab at the cell surface, we evaluated the spatial distribution of A488-IgE bound to FcεRI by confocal imaging. For this experiment, as for the flow cytometry measurements, cells were sensitized with A488-IgE, then stimulated or not with antigen for 10 minutes at 37°C in the presence or absence of PAO or quercetin. Cells were then fixed and labeled with anti-Alexa488 and a secondary Ab. As shown in Fig. 3C, top panel, anti-Alexa488 uniformly labels the plasma membrane, and binding of this antibody substantially quenches A488-IgE fluorescence there. Crosslinking of A488-IgE by antigen causes endocytosis of a large percentage of IgE-receptor complexes that are distributed throughout the cytoplasm and are thereby inaccessible to labeling by anti-Alexa488 and secondary Ab (Fig. 3C, second panel from top). A small percentage of A488-IgE remains at the PM, and its labeling by anti-Alexa488 (red) is dimly visible in membrane ruffles. Treatment with either PAO or quercetin prior to antigen addition does not alter the uniform distribution of A488-IgE at the PM, appearing similar to the top panel in Fig. 3C (D. Holowka, data not shown). However, addition of antigen in the presence of these inhibitors results in a patchy distribution of A488-IgE that is mostly at the PM but poorly labeled by anti-Alexa fluor 488 (Fig. 3C, bottom two panels). Close examination of the distributions of green A488-IgE and red anti-Alexa488 reveals that these are largely noncoincidental, although their distributions are both PM localized. These results suggest that both PAO and quercetin permit formation of endosomal invaginations caused by antigen that fail to pinch off from the plasma membrane. Consistent with this interpretation, we find that the fluorescence of crosslinked FITC-IgE is sensitive to rapid changes in extracellular pH in the presence but not in the absence of these inhibitors (A. Singhai et al., manuscript in preparation).

PAO and Quercetin Inhibit New Synthesis of PI(4,5)P$_2$ at the PM. To directly characterize the effects of PAO and quercetin on PI(4,5)P$_2$ synthesis, we monitored the dynamics of PI(4,5)P$_2$ pools at the PM by using the PH domain of PLCδ1, which is highly specific for PI(4,5)P$_2$ (Stauffer et al., 1998; Várnai and Balla, 1998). RBL cells transiently transfected with a plasmid encoding PLCδ1 PH-EGFP exhibited a homogeneous distribution of this protein at the PM due to the predominant localization of PI(4,5)P$_2$ at this membrane (Várnai and Balla, 1998). Stimulation with antigen for 5 minutes at 37°C results in a reduction of the ratio of PLCδ1 PH-EGFP at the PM to that in the cytoplasm of ~35%, likely due to the activation of PLCγ. In an attempt to inhibit hydrolysis of PI(4,5)P$_2$ to reveal stimulated net synthesis, we added the general inhibitor of PLC, U73122, prior to antigen stimulation, but no net increase in PLCδ1 PH-EGFP at the plasma membrane was observed (Supplemental Fig. 5). As an alternative strategy, we chose to monitor PI(4,5)P2 synthesis after hydrolysis of PI(4,5)P2 stimulated by A23187 activation of PLC, followed by the initiation of net synthesis when extracellular Ca^{2+} is chelated by EGTA (Varnai and Balla, 1998).

As shown in Fig. 4 for two representative RBL cells, treatment with the Ca^{2+} ionophore A23187 activates PLC, resulting in hydrolysis of PI(4,5)P$_2$, which causes substantial translocation of the PH domain from the PM to the cytoplasm in a subset of cells as previously reported for NIH 3T3 cells (Várnai and Balla, 1998). Surprisingly, as shown in Fig. 4, new synthesis of PI(4,5)P$_2$ monitored by PLCδ1 PH-EGFP often occurs as micron-sized patches near the PM. These patches became evident within 1 minute of EGTA addition and remained in the same locations during the imaging time course (8–10 minutes). In addition, a more uniform distribution of PLCδ1 PH-EGFP became evident at the plasma membrane after 5–8 minutes. Interestingly, the PM marker, Alexa fluor 555-cholera toxin B (A555-CTxB) bound to the ganglioside GM$_1$, which initially exhibits a uniform distribution along the PM, also showed some concentration with PLCδ1 PH-EGFP at the PM-proximal patches to varying extents following EGTA addition (Fig. 4).

To test for the capacity of PAO and quercetin to interfere with PI(4,5)P$_2$ resynthesis after A23187-induced PI(4,5)P$_2$ hydrolysis, cells were treated for 5 minutes with these inhibitors prior to addition of EGTA. In cells treated with PAO, newly synthesized PI(4,5)P$_2$ reappeared uniformly along the PM as detected by PLCd1 PH-EGFP, but less brightly than in the unstimulated (resting) cells. Interestingly, an additional accumulation of PLCδ1 PH-EGFP occurred in a perinuclear structure reminiscent of the Golgi complex following addition of EGTA (Fig. 5A). Confocal images of fixed cells labeled with an antibody to the *cis*-Golgi marker GM-130 show partial colocalization of this protein with PI(4,5)P$_2$ marked by PLCδ1 PH-EGFP in this region (Fig. 5B). Comparison of the results presented in Figs. 4 and 5 provide evidence that PAO alters the extent and subcellular distribution of newly synthesized pools of PI(4,5)P$_2$.

For cells treated with quercetin, PI(4,5)P$_2$ resynthesis at or near the PM was also diminished compared with unstimulated cells, but without noticeable appearance of PI(4,5)P$_2$ at or near the Golgi complex (Fig. 6A). As for cells treated with only A23187 and EGTA, some cells with quercetin exhibit localized resynthesis in puncta near the plasma membrane (compare Fig. 6A with Fig. 4). To quantitatively assess the effects PAO and quercetin on new synthesis of PI(4,5)P$_2$ at the plasma membrane, we measured the ratio of PLCδ1 PH-EGFP at the plasma membrane to that in the cytoplasm in
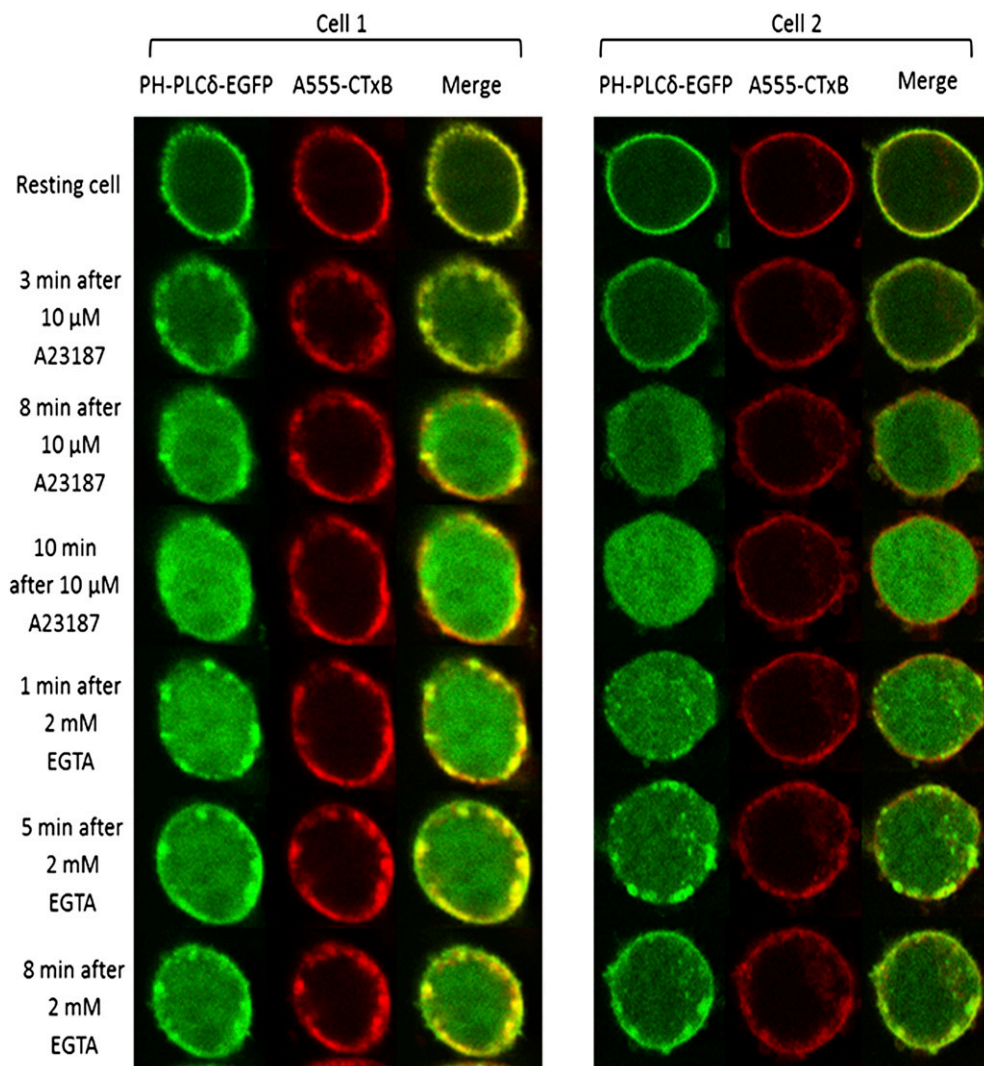
Fig. 4. Newly synthesized $PI(4,5)P_2$ appears in patches at or near the PM. RBL mast cells expressing PLCδ PH-GFP and labeled with A555-CTxB were stimulated with 10 μM A23187, and hydrolysis of $PI(4,5)P_2$ was detected as loss of PLCδ PH-GFP from the plasma membrane. Addition of excess EGTA permits resynthesis to be detected, initially as redistribution of the $PI(4,5)P_2$ reporter to micron-sized patches at or near the plasma membrane. Equatorial confocal microscopy images for two representative cells are shown at indicated time points. Diameters of cells are each ~10 μm.

multiple cells as described in *Materials and Methods*. As summarized in Fig. 6B, we find that 2 μM PAO inhibits new synthesis of $PI(4,5)P_2$ by ~30% and 20 μM quercetin inhibits this by ~60%. These inhibitory effects on resynthesis of $PI(4,5)P_2$ following Ca^{2+}-dependent hydrolysis provide direct evidence for the capacity of PAO and quercetin to inhibit $PI(4,5)P_2$ synthesis under conditions in which they inhibit Ca^{2+} mobilization and other cellular responses mediated by IgE receptors.

Discussion

The pleiotropic roles of $PI(4,5)P_2$ prompted us to search for inhibitors of phosphoinositide synthesis to better characterize its contributions to FcεRI signaling in mast cells. In this study, we found that PAO and quercetin rapidly inhibit Ca^{2+} responses to antigen and interfere with antigen-stimulated cell ruffling and spreading. Moreover, these agents also prevent crosslink-dependent IgE/FcεRI internalization by inhibiting IgE/FcεRI-containing endosomes from pinching off at the PM. Live-cell imaging of the $PI(4,5)P_2$ reporter PH-PLCδ1-EGFP allowed visualization of resynthesized $PI(4,5)P_2$ at or near the PM as micron-sized patches that fail to form

in the presence of PAO. We found that both PAO and quercetin inhibit resynthesis of $PI(4,5)P_2$ at the PM in this assay. Although both PAO and quercetin are known to inhibit other enzyme activities, including tyrosine phosphatases and kinases, respectively, our results and those of Adamczewski et al. (1992) provide evidence that the signaling consequences observed cannot be accounted for by inhibition of these enzyme classes. Our results can be accounted for by inhibition of PI(4)P synthesis by PAO and by inhibition of $PI(4,5)P_2$ synthesis by quercetin to dynamically regulate FcεRI signaling in mast cells.

A previous study provided evidence for PI4KIIIα as the PI4-kinase most important for the generation of $PI(4,5)P_2$ pools at the PM that maintain Ca^{2+} signaling by angiotensin II in HEK-293 cells stably expressing AT_{1a} angiotensin receptors (Balla et al., 2008). This conclusion was based largely on the more potent inhibition by PAO of PI4KIIIα than of PI4KIIIβ or other PI4-kinases in in vitro assays. Our results suggest a dynamic role for PI4KIIIα in Ca^{2+} signaling in mast cells, as antigen-stimulated Ca^{2+} mobilization is rapidly inhibited by low micromolar concentrations of PAO, consistent with the potent inhibition of PI4KIIIα by this compound (Balla et al., 2008). Adamczewski et al. (1992) observed that PAO potently
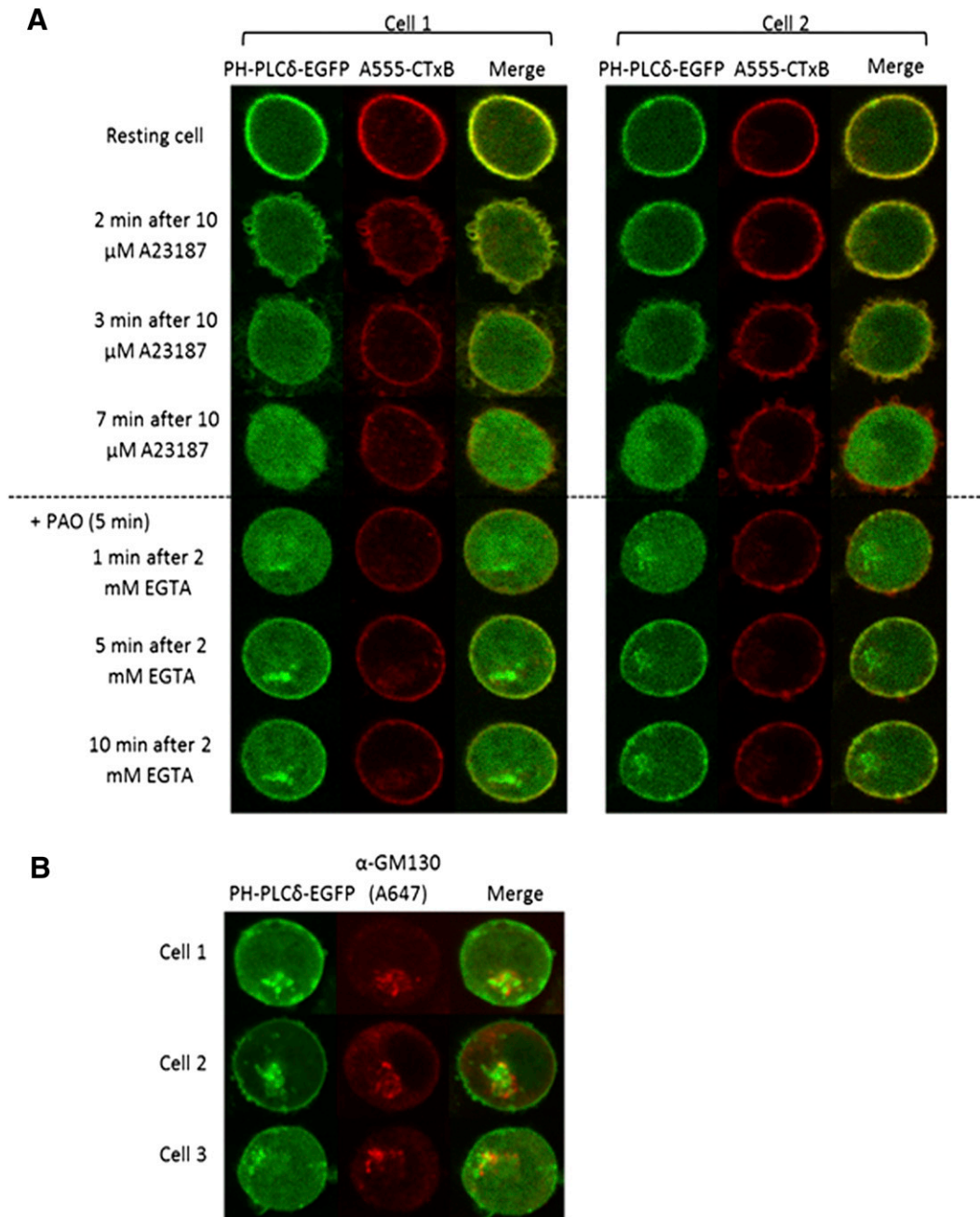
Fig. 5. PAO added just prior to EGTA causes reduction in new synthesis of PI(4,5)P$_2$ at the PM but results in the appearance of a perinuclear pool at or near the Golgi complex. (A) After A23187-induced PI(4,5)P$_2$ hydrolysis, monitored by the translocation of PLCδ PH-GFP from the PM to the cytosol, addition of 2 μM PAO prior to EGTA shows reappearance of fluorescence at the PM and Golgi region. Two representative cells are shown. (B) Cells treated as in (A) were fixed and labeled for the *cis*-Golgi marker GM-130 and confocal microscopy images were obtained. Diameters of cells are each ~10 μm.

inhibits PLCγ1 tyrosine phosphorylation, and they interpreted this to indicate inhibition of a unique pathway for tyrosine phosphorylation of this lipase. However, a subsequent study showed that this PLC isozyme is selectively dependent on PI3-kinase activation (Barker et al., 1998). Thus, the mechanism for PLC inhibition by PAO may well depend on direct or indirect inhibition of PI(3,4,5)P$_3$ synthesis. To evaluate whether inhibition of PI(3,4,5)P$_3$ synthesis could account for the inhibition of antigen-stimulated Ca^{2+} mobilization by PAO or quercetin, we compared their capacities to cause displacement from the PM of the PI(3,4,5)P$_3$-selective PH domain from Akt to that of 200 nM wortmannin,

a specific inhibitor of PI3-kinases at this dose (Yano et al., 1993). As shown in Supplemental Fig. 6, 200 nM wortmannin causes >90% displacement of Akt PH-EGFP from the PM, whereas 2 μM PAO and 20 μM quercetin cause 67 and 77% displacement, respectively. In contrast, 200 nM wortmannin causes <40% inhibition of antigen-stimulated Ca^{2+} responses (Sil et al., 2007; unpublished data), whereas 2 μM PAO and 20 μM quercetin cause ~70% inhibition. Together, these results show that both PAO and quercetin can inhibit PI3-kinases, but this inhibition alone is not likely to account for their inhibition of antigen-stimulated Ca^{2+} mobilization.
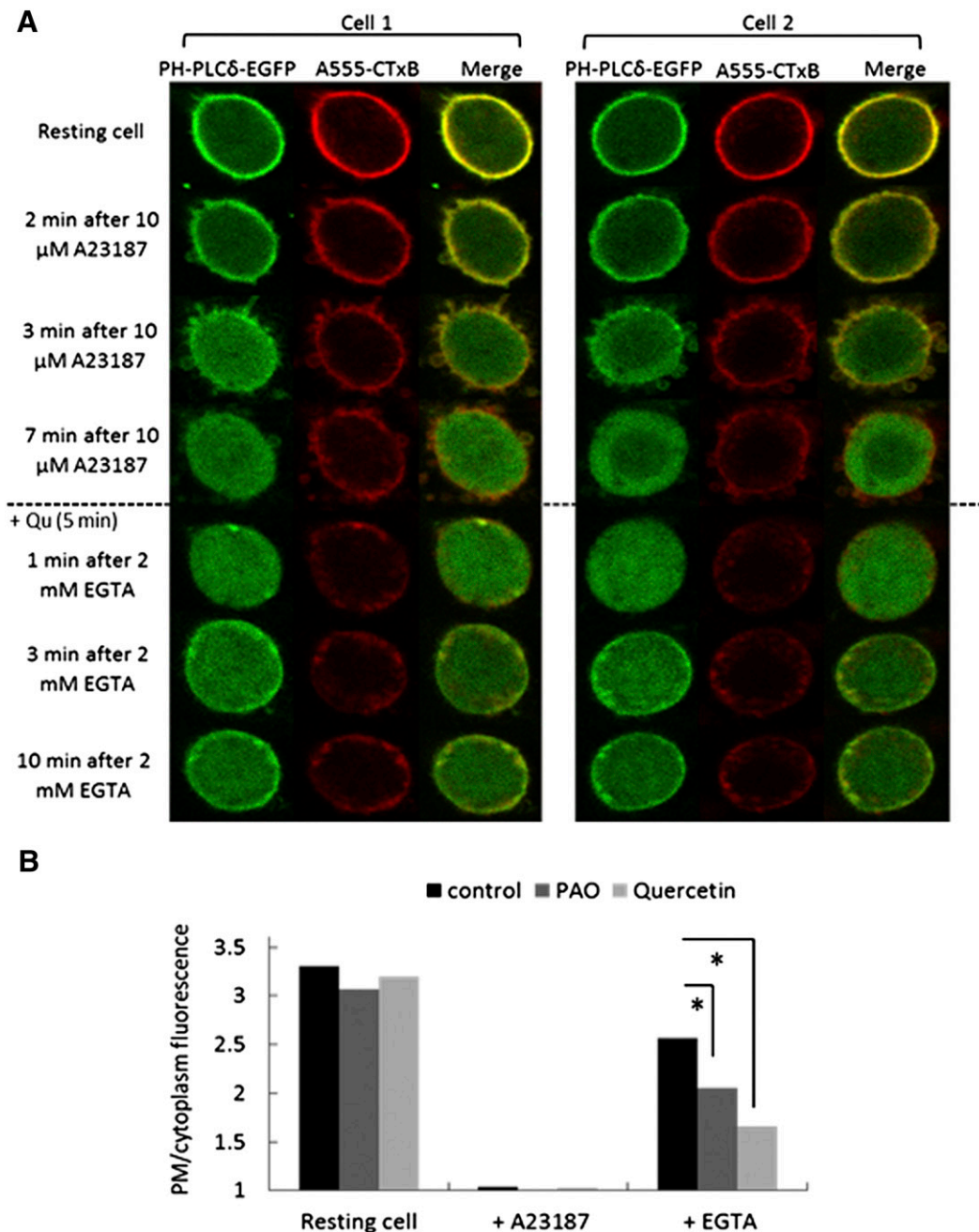
Fig. 6. Quercetin added prior to EGTA causes reduction in new synthesis of PI(4,5)P$_2$ at the PM. (A) After A23187-induced PI(4,5)P$_2$ hydrolysis, monitored by the translocation of PLCδ PH-GFP from the PM to the cytoplasm, RBL cells were treated with 20 μM quercetin for 5 minutes prior to Ca^{2+} chelation with EGTA. Two representative cells are shown. Diameters of cells are each ~10 μm. (B) Quantification for resynthesis of PI(4,5)P$_2$ at the PM. Plots show ratios of the PLCδ PH-GFP fluorescence at the PM to that in the adjacent cytoplasm, determined as described in *Materials and Methods*. Control cells were treated with A23187 followed by EGTA without PAO or quercetin. For each condition, 30 cells were quantified from at least four independent experiments and error bars show S.D. *$P < 0.05$.

Although PAO does not inhibit thapsigargin-stimulated SOCE when added acutely (Fig. 1B), it does cause substantial inhibition when added at least 10 minutes prior to stimulation by thapsigargin (Supplemental Fig. 3), consistent with its capacity to inhibit new PI(4,5)P$_2$ synthesis by depleting the steady-state pool of PI4P. Similarly, wortmannin at concentrations of 10–20 μM is known to inhibit both PI(4)K IIIα and β (Balla and Balla, 2006), and it has been shown to cause substantial inhibition of thapsigargin-stimulated SOCE in RBL mast cells when added at least 10 minutes prior to

stimulation (Broad et al., 2001; Calloway et al., 2011). Under these conditions, it also inhibits coupling between STIM1 and Orai1 (Korzeniowski et al., 2009; Calloway et al., 2011). This prolonged incubation time required for inhibition of SOCE by both wortmannin and PAO is likely due to the need to consume the pool of PI4P at the plasma membrane before inhibition becomes apparent (Balla et al., 2008).

In contrast to these PI4K inhibitors, quercetin causes rapid inhibition of thapsigargin-stimulated Ca^{2+} responses when added after stimulation was initiated (Fig. 1B). This result

suggests that quercetin has a more direct effect on PI(4,5)P$_2$ pools important for SOCE, consistent with a capacity to inhibit PI(4,5)P$_2$ synthesis directly. We previously showed that the polybasic effector domain of the MARCKS protein can serve as an effective monitor of phosphoinositide levels at the PM (Smith et al., 2010; Gadi et al., 2011). Consistent with their capacities to inhibit phosphoinositide synthesis, both quercetin and PAO cause displacement of the MARCKS effector domain from the PM under conditions in which they inhibit SOCE (Supplemental Fig. 7).

The involvement of PI(4,5)P$_2$ in the regulation of cellular actin assembly has been implicated in multiple studies (Honda et al., 1999; Janmey et al., 1999). PI(4,5)P$_2$ does not directly regulate actin polymerization, but rather it interacts with a variety of actin binding proteins to regulate this process (Yin and Janmey, 2003). Consistent with this role, we found that inhibition of PI(4,5)P$_2$ synthesis by quercetin and PAO impairs antigen-stimulated formation of PM ruffles and cell spreading (Fig. 2). The strong inhibitory effect of low doses of PAO on such morphologic changes is consistent with a role for PI(4,5)P$_2$ pools derived from PI4KIIIα activity in regulation of actin polymerization in these events.

Clathrin-mediated endocytosis is the most thoroughly studied example of receptor endocytosis (Schmid and McMahon, 2007), but a number of studies have established the existence of clathrin-independent receptor endocytosis (Mayor and Pagano, 2007). Lamaze et al. (2001) showed that IL-2 receptors of lymphocytes are efficiently internalized despite the inhibition of the clathrin-endocytic machinery, and Sauvonnet et al. (2008) demonstrated that the γc cytokine receptor is also internalized by clathrin-independent endocytosis. These receptors were found to localize in detergent-resistant PM domains that depend on ordered lipid structure. Similarly, FcεRI has been shown to localize in these ordered lipid domains upon antigen-mediated crosslinking (Field et al., 1997). Consistent with this, endocytosis of crosslinked FcεRI receptors was shown to use a nonclathrin-mediated pathway, and FcεRI remains associated with detergent-resistant membranes during endocytosis (Fattakhova et al., 2006).

Although a role for PI(4,5)P$_2$ in clathrin-mediated endocytosis is well established (Di Paolo et al., 2004; Zoncu et al., 2007), our results suggest that it is also important for clathrin-independent endocytosis. We find that PAO and quercetin prevent crosslinked FcεRI-receptors from pinching off from the PM (Fig. 3) at the same doses that inhibit new PI(4,5)P2 synthesis (Figs. 5 and 6). Pinching off of endocytic vesicles from the PM is regulated by dynamin, which contains a PI(4,5)P$_2$-specific PH domain, in addition to a carboxy-terminal proline-rich/arginine-rich domain that directly binds to SH3 domains of actin-associated proteins (Orth and McNiven, 2003). The effects of PAO and quercetin on antigen-induced actin cytoskeletal remodeling leading to morphologic changes and their effects on endocytosis of aggregated FcεRI receptors suggest common molecular targets in these processes.

By using PLCδ1 PH-EGFP to monitor PM-associated PI(4,5)P$_2$, we were unable to find conditions in which antigen stimulation causes a net increase in PM-associated PI(4,5)P$_2$, likely because of the tight coupling of PI(4,5)P$_2$ synthesis to its stimulated hydrolysis. As an alternative strategy, we stimulated PI(4,5)P$_2$ hydrolysis using the Ca^{2+} ionophore A23187 to activate PLC, followed by excess EGTA to chelate extracellular Ca^{2+} and thereby initiate net synthesis of PI(4,5)P$_2$ (Varnai and Balla, 1998). Under these conditions, de novo synthesized PI(4,5)P$_2$ detected by PLCδ1 PH-EGFP appeared initially in the form of large and stable patches localized near the PM, followed by a rim of more uniform PLCδ1 PH-EGFP fluorescence at later times (Fig. 4). These distributions are reminiscent of the so called "PIK patches" that are cortical clusters containing the PI4-kinase Stt4p that are localized to ER-PM junctions in yeast (Baird et al., 2008).

Interestingly, we found that the cortical patches of PI(4,5)P$_2$ also became labeled with fluorescent cholera toxin B that was prebound to ganglioside GM$_1$ at the PM prior to initiation of PI(4,5)P$_2$ hydrolysis. This result suggests that the labeled CTxB, acting as a sensor of membrane curvature, may endocytose at these sites in response to new PI(4,5)P$_2$ synthesis. Hope and Pike (1996) provided evidence for a pool of PI(4,5)P$_2$ associated with detergent-resistant ordered lipids that could be relevant for these observations. Other observations that may be related are those of Johnson et al. (2008), who found that reduced PI(4,5)P$_2$ levels in detergent-resistant membrane fractions caused by targeting an inositol 5'-phosphatase to ordered lipid domains resulted in inhibition of PM ruffling and filopodia formation. Further studies will be necessary to determine the relationship between the cortical PI(4,5)P$_2$ patches, PM domains, and the actin cytoskeleton.

In the presence of PAO and quercetin, resynthesis of PI(4,5)P$_2$ is detected less frequently in cortical patches, and its more uniform accumulation at the PM is reduced compared with control cells (Fig. 6B). Interestingly, in PAO-treated cells, resynthesis of PI(4,5)P$_2$ was frequently seen in the vicinity of the Golgi complex, sometimes subsequent to the appearance of new PI(4,5)P$_2$ at the plasma membrane (Fig. 5; unpublished data). Godi et al. (1999) have shown that PI4KIIIβ, primarily localized to the Golgi complex, together with an unidentified PIP5K that is recruited to the Golgi by Arf1, can generate PI(4)P and PI(4,5)P$_2$, which are implicated in the maintenance of the structural integrity of this organelle.

In summary, our results are consistent with a minimal model in which dynamic regulation of IgE receptor signaling is inhibited by PAO and quercetin via their capacity to inhibit phosphoinositide synthesis in RBL mast cells. On the basis of our findings, these compounds should be useful for exploring roles for phosphoinositide synthesis in other signaling contexts. Although PAO has additional inhibitory effects on tyrosine phosphatases, this other activity generally enhances IgE receptor signaling, and thus can be distinguished from its inhibitory effect on PI4P synthesis. Quercetin has inhibitory effects on stimulated tyrosine phosphorylation, but in RBL mast cells these occur at higher concentrations than those necessary for inhibition of PI-kinases. As a complement to molecular genetic experiments, these compounds provide a useful starting point for understanding the multiple and often complex roles of phosphoinositide synthesis in cell signaling.

Authorship Contributions

Participated in research design: Santos, Holowka, Baird.
Conducted experiments: Santos, Holowka.
Contributed new reagents or analytic tools: Naal, Holowka, Baird.
Wrote or contributed to the writing of the manuscript: Santos, Naal, Holowka, Baird.

References

Adamczewski M, Paolini R, and Kinet JP (1992) Evidence for two distinct phosphorylation pathways activated by high affinity immunoglobulin E receptors. *J Biol Chem* **267**:18126–18132.

Balla A and Balla T (2006) Phosphatidylinositol 4-kinases: old enzymes with emerging functions. *Trends Cell Biol* **16**:351–361.

Balla A, Kim YJ, Varnai P, Szentpetery Z, Knight Z, Shokat KM, and Balla T (2008) Maintenance of hormone-sensitive phosphoinositide pools in the plasma membrane requires phosphatidylinositol 4-kinase IIIalpha. *Mol Biol Cell* **19**:711–721.

Balla A, Tuymetova G, Barshishat M, Geiszt M, and Balla T (2002) Characterization of type II phosphatidylinositol 4-kinase isoforms reveals association of the enzymes with endosomal vesicular compartments. *J Biol Chem* **277**:20041–20050.

Balla T, Szentpetery Z, and Kim YJ (2009) Phosphoinositide signaling: new tools and insights. *Physiology (Bethesda)* **24**:231–244.

Baird D, Stefan C, Audhya A, Weys S, and Emr SD (2008) Assembly of the PtdIns 4-kinase Stt4 complex at the plasma membrane requires Ypp1 and Efr3. *J Cell Biol* **183**:1061–1074.

Barker SA, Caldwell KK, Pfeiffer JR, and Wilson BS (1998) Wortmannin-sensitive phosphorylation, translocation, and activation of PLCgamma1, but not PLCgamma2, in antigen-stimulated RBL-2H3 mast cells. *Mol Biol Cell* **9**:483–496.

Beaven MA (2009) Our perception of the mast cell from Paul Ehrlich to now. *Eur J Immunol* **39**:11–25.

Benhamou M, Ryba NJP, Kihara H, Nishikata H, and Siraganian RP (1993) Protein-tyrosine kinase p72syk in high affinity IgE receptor signaling. Identification as a component of pp72 and association with the receptor gamma chain after receptor aggregation. *J Biol Chem* **268**:23318–23324.

Berridge MJ, Dawson RM, Downes CP, Heslop JP, and Irvine RF (1983) Changes in the levels of inositol phosphates after agonist-dependent hydrolysis of membrane phosphoinositides. *Biochem J* **212**:473–482.

Broad LM, Braun FJ, Lievremont JP, Bird GS, Kuroaki T, and Putney JW, Jr (2001) Role of the phospholipase C-inositol 1,4,5-trisphosphate pathway in calcium release-activated calcium current and capacitative calcium entry. *J Biol Chem* **276**:15945–15952.

Calloway N, Owens T, Corwith K, Rodgers W, Holowka D, and Baird B (2011) Stimulated association of STIM1 and Orai1 is regulated by the balance of PtdIns (4,5)P₂ between distinct membrane pools. *J Cell Sci* **124**:2602–2610.

Cantley LC (2002) The phosphoinositide 3-kinase pathway. *Science* **296**:1655–1657.

Chirumbolo S (2010) The role of quercetin, flavonols and flavones in modulating inflammatory cell function. *Inflamm Allergy Drug Targets* **9**:263–285.

Di Paolo G and De Camilli P (2006) Phosphoinositides in cell regulation and membrane dynamics. *Nature* **443**:651–657.

Di Paolo G, Moskowitz HS, Gipson K, Wenk MR, Voronov S, Obayashi M, Flavell R, Fitzsimonds RM, Ryan TA, and De Camilli P (2004) Impaired PtdIns(4,5)P2 synthesis in nerve terminals produces defects in synaptic vesicle trafficking. *Nature* **431**:415–422.

Fattakhova G, Masilamani M, Borrego F, Gilfillan AM, Metcalfe DD, and Coligan JE (2006) The high-affinity immunoglobulin-E receptor (FcepsilonRI) is endocytosed by an AP-2/clathrin-independent, dynamin-dependent mechanism. *Traffic* **7**:673–685.

Fewtrell CMS and Gomperts BD (1977) Effect of flavone inhibitors of transport ATPases on histamine secretion from rat mast cells. *Nature* **265**:635–636.

Field KA, Holowka D, and Baird B (1997) Compartmentalized activation of the high affinity immunoglobulin E receptor within membrane domains. *J Biol Chem* **272**:4276–4280.

Furuichi K, Rivera J, Buonocore LM, and Isersky C (1986) Recycling of receptor-bound IgE by rat basophilic leukemia cells. *J Immunol* **136**:1015–1022.

Furuichi K, Rivera J, and Isersky C (1984) The fate of IgE bound to rat basophilic leukemia cells. III. Relationship between antigen-induced endocytosis and serotonin release. *J Immunol* **133**:1513–1520.

Gadi D, Wagenknecht-Wiesner A, Holowka D, and Baird B (2011) Sequestration of phosphoinositides by mutated MARCKS effector domain inhibits stimulated Ca$^{(2+)}$ mobilization and degranulation in mast cells. *Mol Biol Cell* **22**:4908–4917.

Godi A, Pertile P, Meyers R, Marra P, Di Tullio G, Iurisci C, Luini A, Corda D, and De Matteis MA (1999) ARF mediates recruitment of PtdIns-4-OH kinase-β and stimulates synthesis of PtdIns(4,5)P₂ on the Golgi complex. *Nat Cell Biol* **1**:280–287.

Hamawy MM, Oliver C, Mergenhagen SE, and Siraganian RP (1992) Adherence of rat basophilic leukemia (RBL-2H3) cells to fibronectin-coated surfaces enhances secretion. *J Immunol* **149**:615–621.

Holowka D, Sil D, Torigoe C, and Baird B (2007) Insights into immunoglobulin E receptor signaling from structurally defined ligands. *Immunol Rev* **217**:269–279.

Honda A, Nogami M, Yokozeki T, Yamazaki M, Nakamura H, Watanabe H, Kawamoto K, Nakayama K, Morris AJ, and Frohman MA et al. (1999) Phosphatidylinositol 4-phosphate 5-kinase α is a downstream effector of the small G protein ARF6 in membrane ruffle formation. *Cell* **99**:521–532.

Hope HR and Pike LJ (1996) Phosphoinositides and phosphoinositide-utilizing enzymes in detergent-insoluble lipid domains. *Mol Biol Cell* **7**:843–851.

Janmey PA, Xian W, and Flanagan LA (1999) Controlling cytoskeleton structure by phosphoinositide-protein interactions: phosphoinositide binding protein domains and effects of lipid packing. *Chem Phys Lipids* **101**:93–107.

Johnson CM, Chichili GR, and Rodgers W (2008) Compartmentalization of phosphatidylinositol 4,5-bisphosphate signaling evidenced using targeted phosphatases. *J Biol Chem* **283**:29920–29928.

Korzeniowski MK, Popovic MA, Szentpetery Z, Varnai P, Stojilkovic SS, and Balla T (2009) Dependence of STIM1/Orai1-mediated calcium entry on plasma membrane phosphoinositides. *J Biol Chem* **284**:21027–21035.

Lamaze C, Dujeancourt A, Baba T, Lo CG, Benmerah A, and Dautry-Varsat A (2001) Interleukin 2 receptors and detergent-resistant membrane domains define a clathrin-independent endocytic pathway. *Mol Cell* **7**:661–671.

Lee HS, Park CS, Lee YM, Suk HY, Clemons TC, and Choi OH (2005) Antigen-induced Ca^{2+} mobilization in RBL-2H3 cells: role of I(1,4,5)P₃ and S1P and necessity of I(1,4,5)P₃ production. *Cell Calcium* **38**:581–592.

Lee J, Veatch SL, Baird B, and Holowka D (2012) Molecular mechanisms of spontaneous and directed mast cell motility. *J Leukoc Biol* **92**:1029–1041.

Ma HT and Beaven MA (2009) Regulation of Ca^{2+} signaling with particular focus on mast cells. *Crit Rev Immunol* **29**:155–186.

Mayor S and Pagano RE (2007) Pathways of clathrin-independent endocytosis. *Nat Rev Mol Cell Biol* **8**:603–612.

Menon AK, Holowka D, Webb WW, and Baird B (1986) Cross-linking of receptor-bound IgE to aggregates larger than dimers leads to rapid immobilization. *J Cell Biol* **102**:541–550.

Middleton E, Jr, Kandaswami C, and Theoharides TC (2000) The effects of plant flavonoids on mammalian cells: implications for inflammation, heart disease, and cancer. *Pharmacol Rev* **52**:673–751.

Naal RMZG, Holowka EP, Baird B, and Holowka D (2003) Antigen-stimulated trafficking from the recycling compartment to the plasma membrane in RBL mast cells. *Traffic* **4**:190–200.

Orth JD and McNiven MA (2003) Dynamin at the actin-membrane interface. *Curr Opin Cell Biol* **15**:31–39.

Paolini R, Jouvin M-H, and Kinet J-P (1991) Phosphorylation and dephosphorylation of the high-affinity receptor for immunoglobulin E immediately after receptor engagement and disengagement. *Nature* **353**:855–858.

Passante E and Frankish N (2009) The RBL-2H3 cell line: its provenance and suitability as a model for the mast cell. *Inflamm Res* **58**:737–745.

Pfeiffer JR, Seagrave JC, Davis BH, Deanin GG, and Oliver JM (1985) Membrane and cytoskeletal changes associated with IgE-mediated serotonin release from rat basophilic leukemia cells. *J Cell Biol* **101**:2145–2155.

Posner RG, Lee B, Conrad DH, Holowka D, Baird B, and Goldstein B (1992) Aggregation of IgE-receptor complexes on rat basophilic leukemia cells does not change the intrinsic activity but can alter the kinetics of the ligand-IgE interaction. *Biochemistry* **31**:5350–5356.

Raucher D, Stauffer T, Chen W, Shen K, Guo S, York JD, Sheetz MP, and Meyer T (2000) Phosphatidylinositol 4,5-bisphosphate functions as a second messenger that regulates cytoskeleton-plasma membrane adhesion. *Cell* **100**:221–228.

Rivera J and Gilfillan AM (2006) Molecular regulation of mast cell activation. *J Allergy Clin Immunol* **117**:1214–1225, quiz 1226.

Sauvonnet N, Dujeancourt A, and Dautry-Varsat A (2005) Cortactin and dynamin are required for the clathrin-independent endocytosis of gammac cytokine receptor. *J Cell Biol* **168**:155–163.

Schmid EM and McMahon HT (2007) Integrating molecular and network biology to decode endocytosis. *Nature* **448**:883–888.

Seldin DC, Adelman S, Austen KF, Stevens RL, Hein A, Caulfield JP, and Woodbury RG (1985) Homology of the rat basophilic leukemia cell and the rat mucosal mast cell. *Proc Natl Acad Sci USA* **82**:3871–3875.

Sil D, Lee JB, Luo D, Holowka D, and Baird B (2007) Trivalent ligands with rigid DNA spacers reveal structural requirements for IgE receptor signaling in RBL mast cells. *ACS Chem Biol* **2**:674–684.

Smith NL, Hammond S, Gadi D, Wagenknecht-Wiesner A, Baird B, and Holowka D (2010) Sphingosine derivatives inhibit cell signaling by electrostatically neutralizing polyphosphoinositides at the plasma membrane. *Self Nonself* **1**:133–143.

Sorkin A and Von Zastrow M (2002) Signal transduction and endocytosis: close encounters of many kinds. *Nat Rev Mol Cell Biol* **3**:600–614.

Stauffer TP, Ahn S, and Meyer T (1998) Receptor-induced transient reduction in plasma membrane PtdIns(4,5)P₂ concentration monitored in living cells. *Curr Biol* **8**:343–346.

Várnai P and Balla T (1998) Visualization of phosphoinositides that bind pleckstrin homology domains: calcium- and agonist-induced dynamic changes and relationship to myo-[³H]inositol-labeled phosphoinositide pools. *J Cell Biol* **143**:501–510.

Vasudevan L, Jeromin A, Volpicelli-Daley L, De Camilli P, Holowka D, and Baird B (2009) The β- and γ-isoforms of type I PIP5K regulate distinct stages of Ca^{2+} signaling in mast cells. *J Cell Sci* **122**:2567–2574.

Vig M and Kinet JP (2009) Calcium signaling in immune cells. *Nat Immunol* **10**:21–27.

Wiedemann C, Schäfer T, and Burger MM (1996) Chromaffin granule-associated phosphatidylinositol 4-kinase activity is required for stimulated secretion. *EMBO J* **15**:2094–2101.

Yano H, Nakanishi H, Kimura K, Hanai N, Saitoh Y, Fukui Y, Nonomura Y, and Matsuda Y (1993) Inhibition of histamine secretion by wortmannin through the blockade of phosphatidylinositol 3-kinase in RBL-2H3 cells. *J Biol Chem* **268**:25846–25856.

Yin HL and Janmey PA (2003) Phosphoinositide regulation of the actin cytoskeleton. *Annu Rev Physiol* **65**:761–789.

Zoncu R, Perera RM, Sebastian R, Nakatsu F, Chen H, Balla T, Ayala G, Toomre D, and De Camilli PV (2007) Loss of endocytic clathrin-coated pits upon acute depletion of phosphatidylinositol 4,5-bisphosphate. *Proc Natl Acad Sci USA* **104**:3793–3798.

Address correspondence to: David Holowka, Department of Chemistry and Chemical Biology, Baker Laboratory, Cornell University, Ithaca, NY 14853-1301. E-mail: dah24@cornell.edu